CrystEngComm



PAPER

View Article Online



Cite this: CrystEngComm, 2023, 25, 4076

Additive controlled packing polymorphism in a series of halogen-substituted dithieno[3,2-a:2',3'c]phenazine derivatives†

Boris B. Averkiev, a Raúl Castañeda, b Marina S. Fonari, bc Evgheni V. Jucov^b and Tatiana V. Timofeeva (1)*b

For a series of substituted dithieno[3,2-a:2',3'-c]phenazine derivatives X-ray diffraction studies have been carried out. It was found that depending on crystallization conditions (solution or gas phase and additives) two or three packing polymorphs were obtained for phenazine derivatives with H, F and Cl substituents. For F-substituted compounds an unusual number of symmetrically independent molecules (six and four) were found among its crystalline polymorphs. Comparison of the calculated lattice energies revealed insignificant energy differences between the polymorphs, thus explaining the existence of the large number of polymorphs in this series of materials. TD-DFT calculations of the HOMO-LUMO gap for these molecules demonstrated close correspondence to the results of previously published electrochemical measurements

Received 19th April 2023, Accepted 10th June 2023

DOI: 10.1039/d3ce00387f

rsc.li/crystengcomm

1. Introduction

Multiple sources tell that in spite of significant efforts invested in studies of polymorphism of molecular crystals, it is still almost impossible to theoretically predict the structure of thermodynamically stable polymorphs from the variety of possible crystalline forms for a particular material and to figure out how to obtain certain polymorphs. Therefore, the famous quotation from McCrone that "the number of forms known for a given compound is proportional to the time and money spent in research on that compound" is still in place and has many supporters.2-5 It is interesting to mention, however, that for many materials a second polymorph was never found, most probably because researchers, after establishing the structure of the material under study, did not attempt a detailed study of material polymorphism. On the other hand, in many cases the second polymorph modification was found long after the first one and was discovered quite unexpectedly when, for instance, the materials under investigation have been crystallized in the presence of another compound. For example, crystals of

maleic acid were characterized as early as 1881 and until 2006, for 124 years, has been considered to be monomorphic.6 However, an attempt to co-crystallize this acid with caffeine brought the discovery of the second form of maleic acid. The appearance of maleic acid form II should serve as a precaution against assuming that consistent production of only one crystal form rules out the appearance of new polymorphs. It was suggested that the presence of an additive (coformer) may have played a structure-directing role in the growth of this latent crystal form.⁴ A similar situation was observed for sym-trinitrobenzene, where two new stable crystal forms of the 120-year-old compound were obtained by applying an additive, trisindane, and changing the thermodynamic conditions of crystal growth.⁷ Other polymorphs may be discovered during exploration of new solvent/co-solute combinations.4 This statement is supported by examples of co-crystallization which enable formation of new polymorphs. For instance, induced conformational polymorphism of 1,1-dicyano-2-(4-hydroxy-3-methoxyphenyl)ethene was observed during attempts to grow its co-crystals with L-proline and L-tartaric acid.8 Co-crystallization of 8-hydroxyquinoline with acetaminophen resulted in a new monoclinic packing polymorph of 8-hydroxyquinoline.9 This effect was discussed in a more general way as additiveinduced polymorphism or additive-controlled crystallization in several reviews. 10-12 Weak interactions such as hydrogen bonding, halogen bonding and other dispersive interactions are reliable and widely used tools that play a crucial role in self-assembly and molecular recognition in the solid state. 13,14

^a Department of Chemistry, Kansas State University, Manhattan, KS 66506, USA

^b Department of Chemistry, New Mexico Highlands University, Las Vegas, NM 87701, USA. E-mail: tvtimofeeva@nmhu.edu

^c Institute of Applied Physics, Moldova State University, Academiei str, 5 MD2028, Chisinau, Republic of Moldova

[†] Electronic supplementary information (ESI) available. CCDC 1576235-1576244. For ESI and crystallographic data in CIF or other electronic format see DOI: https://doi.org/10.1039/d3ce00387f

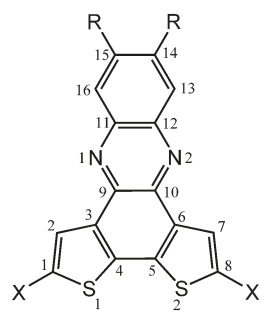
CrystEngComm **Paper**

Polymorphism is especially important for crystal engineering of organic π -conjugated materials, which demonstrate specific intermolecular interactions, including stacking interactions, and every polymorph has specific physical properties useful or preventing their use for organic electronic technology. Molecules in such materials can be arranged in layers or in stacks and different arrangements can alternate physical properties of these materials including their electronic properties. 15-17

Recent findings demonstrating the achievements in the control of polymorphism aimed to show that so far polymorphism has been considered not as a drawback but more as an opportunity that allows control and full exploitation of the intrinsic properties of polymorphism and transitions between its various metastable states, through fine-tuning of molecular packing in a reproducible manner.18-20

Introducing various substituents, such as halogen atoms or bulky groups, allow modulation of intermolecular interactions and molecular packing, making some crystal structures preferable in terms of their properties.²¹

One such property is charge transport in organic semiconductors, which can be altered dramatically in various polymorphs of the same compound due to variation of intermolecular interactions.²² Although some features of molecular arrangement and intermolecular interactions in the charge transfer crystalline polymorphs have been discussed, there is no general approach that can predict these properties based on crystal structure. Accumulation of experimental data will help researchers to move closer to formulation of such an approach. The influence of weak intermolecular interactions on electronic properties in crystalline polymorphs of molecular compounds was studied experimentally and theoretically.23-30 Two polymorphs of 5,11-bis(triethylsilylethynyl)anthradithiophene fluorinated with slightly different packing show different temperature dependence of the charge mobilities.²³ From the two polymorphs of thieno[3,2-b]thiophenethiazolo[5,4-d]thiazole, only a herringbone packed polymorph with continuous π - π stacking and S...S close contacts displayed p-type semiconductive properties, while the polymorph with slipped-stacked packing, in which molecules are arranged in isolated groups of tetramers, is an insulator.26 For these polymorphs, calculations suggest the possibility of an n-type character of conductivity, which was not observed in the experiments. Theoretical calculations of the charge transport properties for three crystalline polymorphs of 9,10-bis((E)-2-(pyrid-2-yl)vinyl)anthracene have shown that the different character of molecular overlapping and intermolecular interactions affect the transfer integrals and reorganization energy in these three polymorphs.²⁷ Calculations using density functional theory and Marcus charge transport theory revealed that different intermolecular interactions in four quinacridone polymorphs impact their hole mobility.²⁸ All four of them can be used as electron transport materials, but only the α^{II} polymorph can be used as dipolar transport



Scheme 1 The structural formula of the studied DTPhz derivatives with the atom numbering scheme; R = H, F, Cl, Br; X = H, TMS.

material. The influence of weak interactions such as hydrogen bonding and $\pi \cdots \pi$ interactions on charge transport in various organic polymorphs was also studied theoretically, where correlations between degree of charge transfer and weak intermolecular interactions in polymorph crystals (Hbonds, stacking) were established.²⁹

Reported in this publication, dithienophenazines (Scheme 1) represent a wide class of novel organic π -conjugated compounds with the same core structure as shown in Scheme 1, but various positions heteroatoms.31-39 These compounds attracted considerable interest as potential materials for diverse applications in organic electronics, such as organic light-emitting diodes (OLEDs)31 as well as pendant groups in donor-acceptor polymers for solar cell application 32-34 in dye-sensitized solar cells, 35-37 and in anion probes. 38 This aromatic system with sp²-hybridized nitrogen atoms might be capable of formation of C-H···N hydrogen bonds, and these had been shown to assist molecular self-assembly and increase charge mobility in thin films.³⁹ Surprisingly, according to the Cambridge Structural Database, only a few crystal structures of compounds with the same core and same positions of heteroatoms as presented in Fig. 1 were reported. The initial goal of this project was the creation of dithienophenazine cocrystals with acceptor molecules, for instance, tetracyanoquinodimethane, to obtain charge transfer materials. Unfortunately, our attempts allowed us to obtain only one cocrystalline material. The structure of the charge transfer cocrystal of dithieno[3,2-a:2',3'-c]phenazine DTPhz (X = H, R = H) with TCNQ was described earlier in ref. 40. Nonetheless, these attempts brought about the formation of three groups of polymorphs. It should be mentioned also that in ref. 41, the synthesis, structure and mechanooptics of pure DTPhz (X = H, R = H) were presented. The obtained 1D crystals revealed very uncommon properties such as elastic bending in combination with efficient transmission of optical signals of different colors that suggest potential use of such materials for crystalline flexible waveguides. A series of **DTPhz** derivatives with R = Hal and X = C_nH_{2n+1} was presented. 42,43 Their structures were modified with halogen substituents and linear alkyl chains of various lengths, and they were used as building blocks to assemble luminescent one-dimensional nano-/microcrystals.

Fig. 1 The crystal packing in α H-DTPhz (a) and β H-DTPhz (b). This and all following figures were prepared using XP program.

In the present paper, molecular and crystal structures in series of halogen- and trimethylsilyl (TMS)-substituted dithieno[3,2-a:2',3'-c]phenazines (Scheme 1) and their polymorphism are considered on the basis of experimental diffraction data.

In addition to experimental structures, theoretical calculations of single molecules and crystal structures were carried out to analyze the electronic characteristics of the molecules, in particular, their HOMO-LUMO gaps and excitation energies. For R-DTPhz derivatives (R = H, F, Cl, Br), quantum chemical and force field calculations of crystal structures were carried out for both experimentally studied polymorphs and some hypothetical polymorphs to investigate the possibility to obtain other polymorphs of these compounds.

Development of a concise multi-gram approach to 2,7-bis(trimethylsilyl)benzo[2,1-*b*:3,4-*b*']dithiophene-4,5-dione (TMS-BDDO) previously allowed for preparation of a series of 2,7-dihalo-BDDO derivatives, which were used to investigate the influence of the halide substituents as well as crystallization conditions on their molecular packing in crystals.44-47 In perspective, it would be possible to cocrystallize the donor molecules presented here with acceptor molecules to engineer charge transfer (CT) materials in the form of cocrystals and thin films. 40,41

2. Materials and methods

Synthesis of materials

The key starting material for the preparation of dithieno[3,2a:2',3'-c]phenazine derivatives, TMS-BDDO, was prepared in two steps commercially available 2-bromothiophene. 45-47 Dithieno[3,2-a:2',3'-c]phenazine derivatives H-DTPHz, F-DTPHz and Cl-DTPHz were prepared in two steps by the condensation reaction of TMS-BDDO with benzene-1,2-diamine derivatives followed by the removal of trimethylsilyl (TMS) groups with tetrabutylammonium fluoride. Detailed descriptions of these procedures are given in ref. 40. The Br-DTPHz derivative was prepared from the unsubstituted condensation **BDDO** with by 4,5-dibromobenzene-1,2-diamine.

Growth of single crystals for X-ray analysis

Crystal growth for X-ray diffraction studies was carried out from solution and from vapor phase. Usually, several solvents were used for material crystallization. Crystallization from dichloromethane (DCM) resulted in needle-shaped yellow a H-DTPhz and α F-DTPhz crystals. The second polymorphs, yellow prism-shaped β H-DTPhz and yellow plate-like β F-DTPhz, were obtained via physical vapor transport (PVT) during attempts to cocrystallize them with TCNQ using this method.⁴⁸ The third polymorph, yellow needles of γ F-DTPhz, was obtained during an attempt to cocrystallize it with TCNQ from dichloromethane solution. Yellow needles of a Cl-DTPhz were crystallized from chloroform solution, and orange blocks of β Cl-DTPhz were crystallized from a 1:1 mixture of toluene and DCM. Orange blocks of Br-DTPhz were crystallized from toluene solution. TMS-F-DTPhz and TMS-Cl-DTPhz were crystallized from chloroform solution.

Single-crystal X-ray diffraction

Single-crystal experiments were carried out with a Bruker SMART diffractometer equipped with an APEX II CCD detector using MoK α (λ = 0.71073 Å) radiation. All singlecrystal diffraction data were integrated using the SAINT software program within the APEX II software suite and absorption corrections were applied using SADABS. 49,50 The TWINABS program was used for y F-DTPhz crystals, which were non-merohedral twins.51 The structures were solved and refined using SHELXTL programs. 52,53 All non-hydrogen atoms were located in difference Fourier maps and were refined anisotropically. Hydrogen atoms were added geometrically and refined with the use of a riding model. Crystal data, data collection and structure refinement details are summarized in Tables 1 and 2. The shortest

Table 1 Selected crystallographic data for R-DTPhz (R = H, F, Cl, Br) derivatives

	α H-DTPhz	β H-DTPhz	α F-DTPhz	β F-DTPhz	γ F-DTPhz	$\alpha \; \text{Cl-DTPhz}$	β Cl-DTPhz	Br-DTPhz
Empirical formula	$C_{16}H_8N_2S_2$	$C_{16}H_{8}N_{2}S_{2}$	$C_{16}H_{6}F_{2}N_{2}S_{2}$	$C_{16}H_{6}F_{2}N_{2}S_{2}$	$C_{16}H_6F_2N_2S_2$	$\mathrm{C}_{16}\mathrm{H}_6\mathrm{Cl}_2\mathrm{N}_2\mathrm{S}_2$	$\mathrm{C}_{16}\mathrm{H}_6\mathrm{Cl}_2\mathrm{N}_2\mathrm{S}_2$	$C_{16}H_6Br_2N_2S_2$
Method,	Solution	PVT,	Solution	PVT, TCNQ	Solution,	Solution,	Solution,	Solution,
solvent, additive	dichloromethane	TCNQ	dichloromethane		dichloromethane, TCNQ	chloroform	toluene/DCM	toluene
Color	Yellowish	Yellow	Yellowish	Yellow	Yellow	Yellow	Light orange	Orange
FW	292.36	292.36	328.35	328.35	328.35	361.25	361.25	450.17
Crystal system	Orthorhombic	Triclinic	Triclinic	Triclinic	Monoclinic	Monoclinic	Orthorhombic	Orthorhombio
Space group	$P2_{1}2_{1}2_{1}$	$P\bar{1}$	$P\bar{1}$	$P\bar{1}$	C2/c	$P2_1/n$	$P2_12_12_1$	$P2_{1}2_{1}2_{1}$
a, Å	4.8175(7)	8.317 (1)	13.536(2)	14.175(4)	26.70(2)	4.9687(7)	9.076(1)	9.034(2)
b, Å	15.993(2)	10.874(2)	15.446(2)	14.277(4)	4.815(3)	18.077(3)	10.183(1)	10.366(2)
c, Å	16.143(2)	14.978(2)	19.582(2)	16.501(4)	20.82(2)	15.442(2)	29.957(4)	30.468(6)
α, °	90	99.580(2)	80.141(2)	112.680(3)	90	90	90	90
β, ∘	90	102.642(2)	84.184(2)	95.238(3)	104.90(1)	92.142(2)	90	90
γ, °	90	101.257(2)	78.220(2)	115.518(3)	90	90	90	90
$V_{\rm calc}$, $\mathring{\rm A}^3$	1243.7(3)	1265.0(3)	3939.3(8)	2644(1)	2586(3)	1386.0(4)	2768.7(6)	2853(1)
Z	4	4	12	8	8	4	8	8
Z'	1	2	6	4	1	1	2	2
$ ho_{ m calc}$, g cm $^{-3}$	1.561	1.535	1.661	1.649	1.687	1.731	1.733	2.096
T, K	100	215	100	215	215	100	215	100
μ^{-1} , mm	0.416	0.409	0.425	0.422	0.431	0.764	0.765	5.970
Unique reflections	3622	8105	20 489	17 407	3758	4257	8042	8357
Unique reflections with $I > 2\sigma(I)$	3354	6740	17 353	12 125	2488	3615	7941	7595
$R_{\rm int}$	0.0485	0.0277	0.0325	0.0404	_	0.0274	0.0188	0.0660
$R_1 (I > 2\sigma(I))$	0.0324	0.0398	0.0608	0.0439	0.0564	0.0325	0.0268	0.0346
$WR_2 (I > 2\sigma(I))$	0.0718	0.1033	0.1499	0.1042	0.1193	0.0783	0.0685	0.0841

Table 2 Selected crystallographic data for TMS-DTPhz derivatives

	TMS-F-DTPhz	TMS-Cl-DTPhz
Empirical formula	C ₂₂ H ₂₂ F ₂ N ₂ S ₂ Si ₂	C ₂₂ H ₂₂ Cl ₂ N ₂ S ₂ Si ₂
Method, solvent	Solution,	Solution,
	chloroform	chloroform
Color	Yellow	Yellow
FW	472.71	505.61
Crystal system	Orthorhombic	Triclinic
Space group	Pnma	$P\bar{1}$
a, Å	26.626(4)	7.3053(19)
<i>b</i> , Å	6.9557(11)	10.911(3)
c, Å	12.568(2)	15.153(4)
α , $^{\circ}$	90	88.935(4)
β , \circ	90	85.183(4)
γ, °	90	82.192(4)
$V_{\rm calc}$, $\mathring{\rm A}^3$	2327.6(6)	1192.4(5)
Z	4	2
Z'	0.5	1
$\rho_{\rm calc}$, g cm ⁻³	1.349	1.408
<i>T</i> , K	215	100
μ^{-1} , mm	0.360	0.561
Unique reflections	3666	5707
Unique reflections with $I >$	2853	4419
$2\sigma(I)$		
$R_{ m int}$	0.0569	0.0298
$R_1 (I > 2\sigma(I))$	0.0459	0.0452
$WR_2 (I > 2\sigma(I))$	0.0640	0.0658

intermolecular contacts as calculated by Mercury⁵⁴ are summarized in Table S1.† Hirshfeld surface analysis and distribution of types of intermolecular interactions within polymorphic series and between structures was carried out using CrystalExplorer17 software⁵⁵ and results are summarized in the ESI† (Fig. S1-S16 and Table S2).

CCDC 1576235-1576244 contains the ESI† crystallographic data for this paper.

Theoretical calculations

Quantum chemical calculations of molecular geometry, HOMO and LUMO energy levels, and excitation energies (TD-DFT method) for DTPhz derivatives were carried out at the B3LYP/6-311G(d) and M06/6-311G(d) levels of theory using the Gaussian09 program.⁵⁶ The initial molecular coordinates were taken from crystallographic data.

The geometries and energies of crystal structures of R-DTPhz polymorphs were calculated using empirical force field and quantum chemical approaches. Force field calculations were done using COMPASS force field implemented in Cerius2 software. 57,58 Quantum chemical calculations were done with the Perdew-Burke-Ernzerhof functional with the addition of a semi-empirical Grimme correction (PBE-D method) and ultra-soft pseudopotentials

(PBE-RRKJUS for C, N, and H, and PBE-N-RRKJUS_PSL for S, F Cl, and Br atoms) implemented in version 5.0.1 of Quantum Espresso program. ^{59–62} The initial geometries were taken from experimental X-ray crystal structures. Full optimization of the unit cell parameters along with all atomic positions was carried out.

3. Results and discussion

Molecular structure

X-ray analysis revealed that the molecules of **R-DTPhz** (R = H, F, Cl, Br) are planar with mean least-square deviation for aromatic core ranging from 0.01 to 0.06 Å. All molecules possess the local C_{2v} symmetry. The molecular geometries of the dithiophene fragment are similar to geometries of this fragment in 52 structures from the Cambridge Structural Database (CSD, Version 5.43, November 2022).⁶³ All four S-C bonds are essentially the same (1.719(2)-1.728(2) Å) and comparable with average values from CSD, 1.725(10) and 1.732(15) Å for S(1)-C(4) (equivalent to S(2)-C(5)) and S(1)-C(1) (equivalent to S(2)-C(8)), respectively. The molecular geometries of the phenazine core are similar to geometries of this fragment in 348 structures from the CSD. For all molecules, the C(9)-C(10) (1.438(4)-1.457(4) Å) bond distances (Scheme 1) are elongated in comparison to the C(11)-C(12) bond (1.415(4)-1.441(4) Å) and an average CSD value of 1.432 (13) Å due to conjugation with the dithiophene fragment. The N(1)-C(9) and N(2)-C(10) bonds (1.328(3)-1.340(3) Å) are slightly shortened in comparison to average values from CSD, 1.344(12) Å, while N(1)-C(11) and N(2)-C(12) bonds (1.343(3)-1.357(3) Å) are slightly elongated. It is also possible to observe bond length alternation in the sixmembered ring C(11)-C(16): bonds C(13)-C(14) and C(15)-C(16), 1.36 Å, are shorter than four other bonds, equal to 1.42 Å. Such an experimentally found bond length distribution corresponds to Scheme 1. The halogen substituents in the F-DTPhz, Cl-DTPhz, and Br-DTPhz molecules do not alter their geometries significantly. Bond lengths in these structures are similar to the corresponding values in H-DTPhz.

In addition to X-ray experiments, quantum chemical calculations (B3LYP/6-311G(d)) and M06/6-311G(d)) of these molecules in the gas phase have been carried out. The calculated molecular geometries are in good agreement with the experimental results. The mean unsigned errors for B3LYP/6-311G(d) and M06/6-311G(d) methods are 0.007 and 0.008 Å, respectively. The largest disagreements were observed for C–S bonds. The calculated S(1)–C(4) bond lengths (X-ray average 1.722 Å) are 1.731 and 1.741 Å for M06 and B3LYP functionals, respectively. The S(1)–C(1) bond lengths (X-ray average 1.725 Å) are 1.738 and 1.746 Å.

For molecules with TMS substituents, **TMS-F-DTPhz** and **TMS-Cl-DTPhz**, the S(1)–C(1) and S(2)–C(8) bonds adjacent to TMS are slightly elongated in comparison to the S(1)–C(4) and S(2)–C(5) bonds. This observation is in agreement with quantum chemical calculations of these

molecules. The aromatic systems in both molecules are planar.

Molecular packing in crystals

In spite of similar molecular shapes, in crystals of the studied compounds, molecules packed differently, demonstrating for three of the materials the so-called packing polymorphs. Thus, seven packing motifs were observed for **R-DTPhz** (R = H, F, Cl, Br) compounds.

For H-DTPhz, two polymorphs with very distinctive crystal packings were obtained by crystallization from solution (orthorhombic) and from vapor phase (triclinic). The orthorhombic a H-DTPhz polymorph contains crystallographically unique molecule. The molecules are packed in stacks along the [1 0 0] direction (Fig. 1a). Each stack contains identical molecules related by translation (Fig. 2) with the interplanar distance equal to 3.38 Å. Of other specific interactions, only weak edge-to-edge CH···N contacts between neighboring stacks were found. The molecules from neighboring stacks related by the twofold screw axis form an interplanar angle of 65.72° and are interconnected by weak CH···N hydrogen bonds [C(13)-H(13)···N2, 3.486(3), 2.73 Å; ∠CHN 137.6°, and C(8)-H(8)···N1, 3.340(3), 2.53 Å; ∠CHN 143.4°, Table S1†].

The triclinic β **H-DTPhz** polymorph (Fig. 1b) contains two crystallographically unique molecules **A** and **B** located in almost perpendicular planes. Molecules **A** are arranged in centrosymmetric stacking dimers (Fig. 3a) with a big overlapping area and an interplanar distance of 3.53 Å. The dimers are stacked in the [1 0 0] direction. Molecules **B** only slightly overlap (Fig. 3b) with an interplanar distance of 3.46 Å, and they do not form stacks. On the other hand, the shortened intermolecular S(1B)···S(2B) contacts of 3.4857(7) Å were registered between adjacent **B** molecules. These contacts link molecules in planar centrosymmetric dimers that are further interlinked as planar tapes through stabilizing H···H contacts, H(13B)···H(14B) = 2.158 Å (Table S1†);⁶⁴ both types

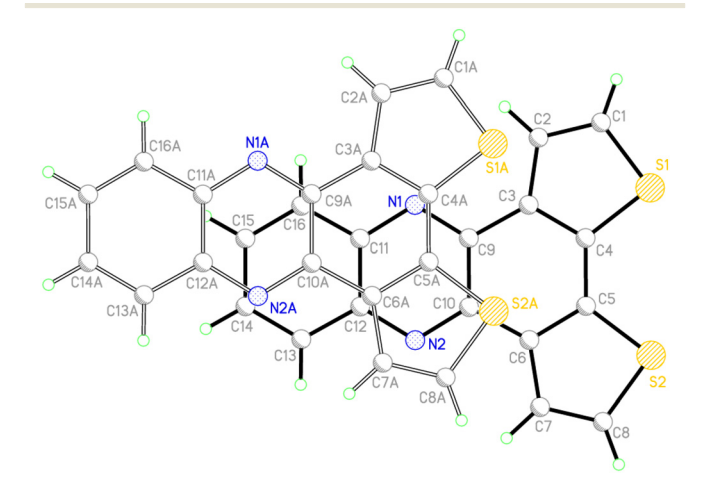


Fig. 2 An overlay scheme of the molecules in stacks of α H-DTPhz. Symmetrically equivalent atoms are denoted with the suffix A.

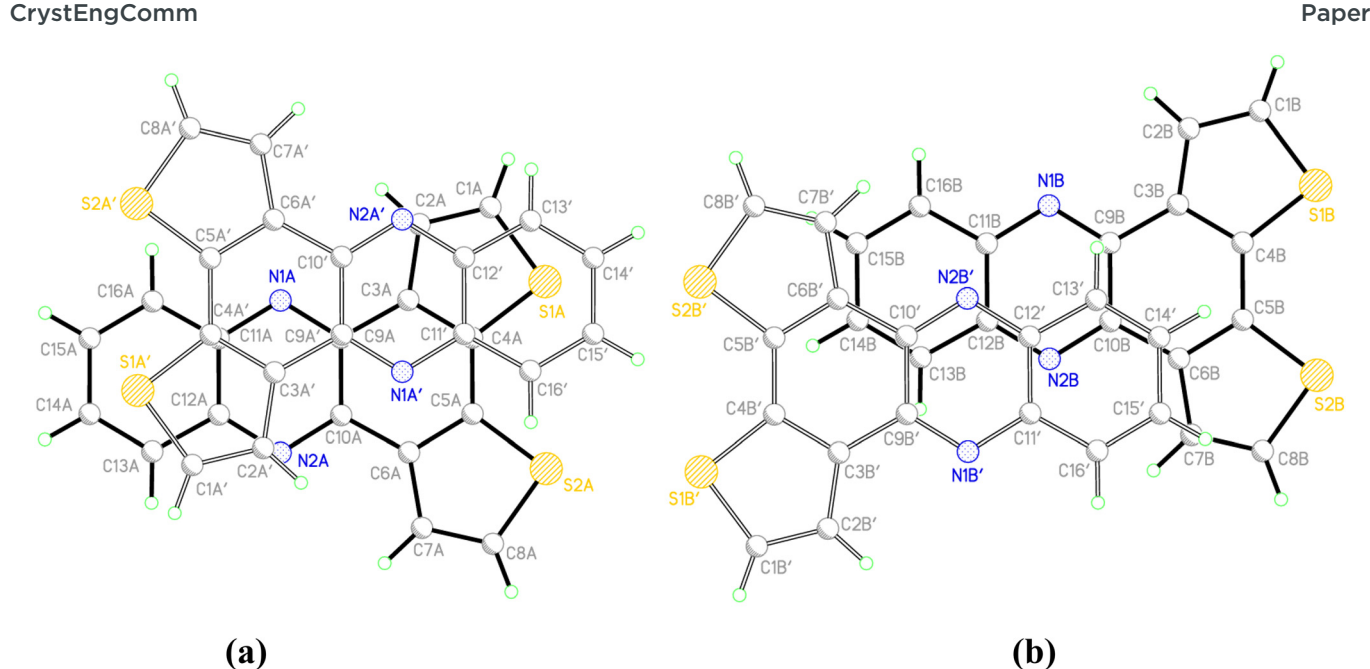


Fig. 3 An overlay scheme of the antiparallel molecules A (a) and B (b) in dimers of β H-DTPhz. The symmetrically equivalent atoms are denoted with the prime symbol.

of interactions are absent in a H-DTPhz. It should be mentioned that α form molecules are packed in a parallel manner, which is different from β modification where they are packed in an antiparallel manner.

Crystallization of F-DTPhz from two solvents and vapor phase produced three crystalline forms of this compound. Since substitution of two hydrogen atoms in the H-DTPhz molecule with two F atoms did not change significantly the molecular shape and volume, it was reasonable to suggest that structures of F-substituted phenazines would be

isomorphic or at least similar to crystal structures of unsubstituted molecules. However, structural similarities were not observed for these derivatives; in contrast, it appeared that F-substituted compounds were quite unique, demonstrating packing in crystals with several systems of symmetrically independent molecules and significant impact of specific F···F, C···F, and CH···F interactions in the crystal packing (Tables S1 and S2 and Fig. S6, S8, and S10†). 65-68

The crystal packing in the triclinic polymorph α F-DTPhz very uncommon; its asymmetric unit contains six

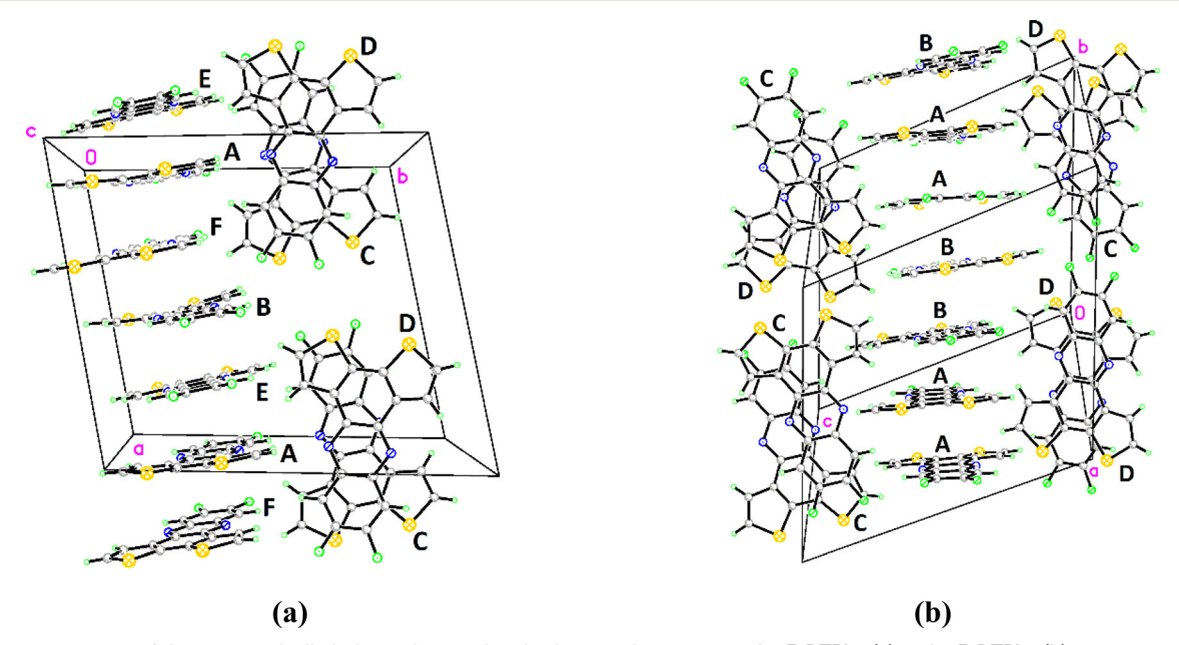


Fig. 4 An arrangement of the symmetrically independent molecules in crystal structures of α F-DTPhz (a) and β F-DTPhz (b).

independent molecules (Fig. 4a). Four molecules, A, B, E, and F, are almost parallel, with the interplanar angles between the plane of molecule A and that of molecules B, E, and F equal to 4.1°, 3.6°, and 3.6°, respectively. These molecules are arranged in stacks along the [1 0 0] direction. The distances between the molecular centroids and the planes of neighboring molecules in the stack vary from 3.3 to 3.5 Å. Two other molecules, C and D, are almost orthogonal to the previous four (for example, C/A and D/A angles are equal to 93.6° and 92.6°) and form a dimer. The angle between molecular planes in the CD dimer is 9.3°. The distance from the centroid of molecule C to the plane of molecule D is 3.4 Å. From specific interactions, the most meaningful contacts are F(2D)···F(1B) 2.744(3) Å, F(2)···N(1C) 2.874 Å, S(2B) ···S(2B) = 3.204(1) Å, S(2A)···S(2A) 3.513 Å, and numerous CH···F contacts (Table S1†).

The crystal of the triclinic polymorph β F-DTPhz, obtained from the vapor phase, contains four symmetrically independent molecules, A, B, C, and D (Fig. 4b). Molecules are arranged into dimers AB and CD (Fig. 5), which are stacked along the [0 1 0] and [1 1 0] directions, respectively. The interplanar angles are 4.2° and 4.1° in dimers AB and CD. In both dimers the distances from the centroid of one molecule to the plane of the second molecule are in the range of 3.4-3.5 Å. The molecules from different dimers are situated in approximately perpendicular positions, but to a lesser extent than that in the \alpha F-DTPhz polymorph. The interplanar angles between molecules from different dimers range from 76.8° to 81.5°. The molecular arrangement in the crystal is somewhat similar to the arrangement in the α F-DTPhz crystal (Fig. 4); however, in the structure of α F-DTPhz, dimers CD do not form infinite stacks but associate in tetramers via edge-to-edge contact, F(2)···S(3) 3.093(2) Å. The set of intermolecular interactions is poorer than that in the α-polymorph (Table S1†) and does not contain F···F short contacts.

The third γ F-DTPhz polymorph (Fig. 6) crystallizes in the monoclinic C2/c group and contains only one molecule in the asymmetric unit. Similar to the α H-DTPhz polymorph, the molecules form translational stacks along the shortest b-axis (Table 1) with an interplanar distance of 3.39 Å (Fig. 7). In both cases the stacks progress along the shortest axes, b in y **F-DTPhz** and a in α **H-DTPhz**, that tells about the similarity of stacks in these two forms. The interplanar angle between molecules from neighboring stacks is 89.9°. Analogously to α H-DTPhz and β F-DTPhz, molecules form planar S···S connected dimers with S···S distances of 3.488(2) and 3.577(2) Å. Centrosymmetric dimers are associated in the planar tapes via centrosymmetric weak contacts H(3)···F(1) 2.63 Å and form stacking walls. No other short edge-to-edge intermolecular interactions were found between stacking walls related by the twofold screw axis.

The monoclinic α Cl-DTPhz contains molecular stacks along the [1 0 0] direction (Fig. 8a). The distance between molecular planes is 3.41 Å (Fig. 9a). Between the neighboring stacks specific C(4)···Cl(2) 3.365(2) Å (Table S1†) contacts were observed. The neighboring stacks pack in a herringbone mode, with an interplanar angle of 87.9° between adjacent molecules.

In the orthorhombic β Cl-DTPhz (Fig. 8b), two independent molecules (A and B) form dimers (Fig. 9b) with an interplanar angle equal to 5.0°. The average distance from the centroid of one molecule to the plane of the second one is 3.25 Å. The dimers are arranged in stacks along the [1 0 0] direction. The interplanar distance between neighboring dimers in stacks is larger than that between dimers inside the stack (average centroid–plane distance is 3.45 Å), and the overlapping area is smaller.

The crystal structure of **Br-DTPhz** is isomorphic to β **Cl-DTPhz**. The interplanar angle in dimers is 4.5°. The distance from the centroid of one molecule to the plane of the second molecule is 3.28 Å. The interplanar distance between

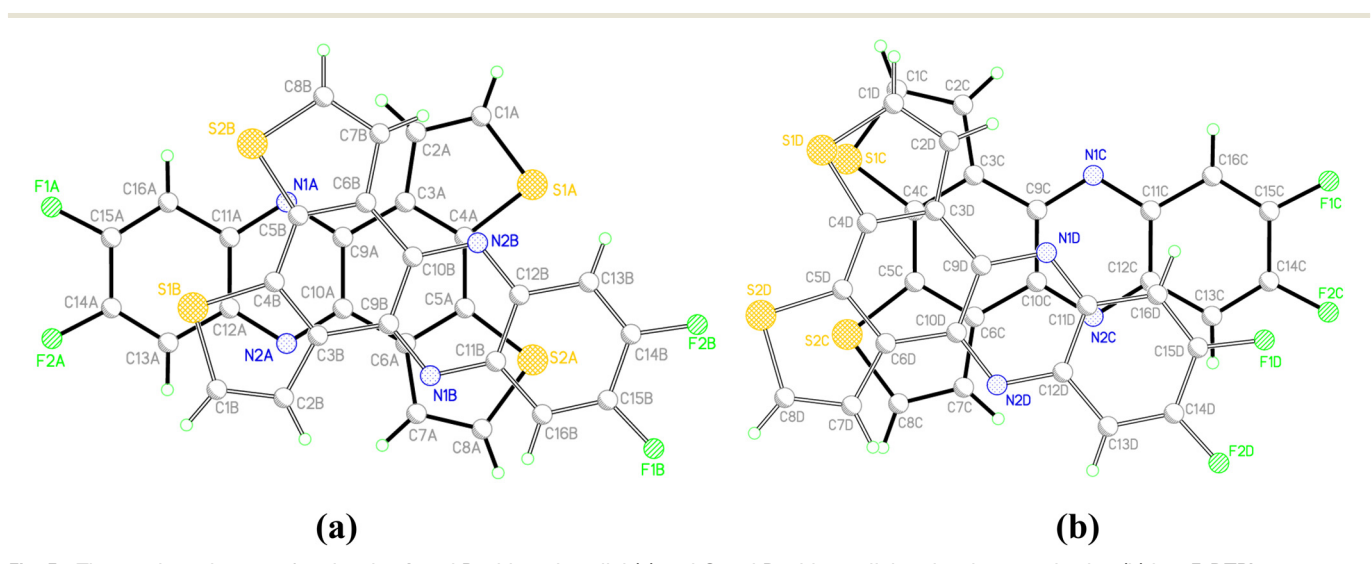


Fig. 5 The overlay schemes of molecules A and B with antiparallel (a) and C and D with parallel molecular organization (b) in β F-DTPhz.

CrystEngComm Paper

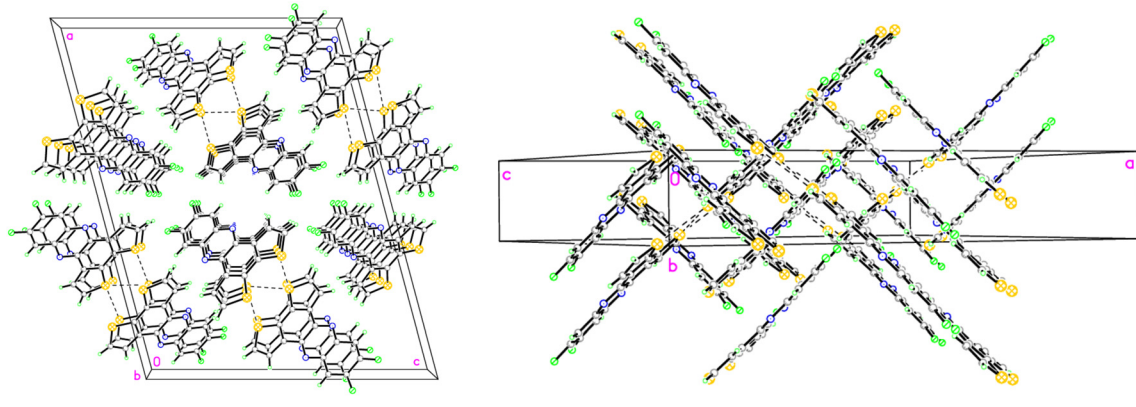


Fig. 6 Crystal packing of γ F-DTPhz in two orientations

neighboring dimers in the stack is larger than that inside the stack (centroid-plane distance is 3.43 Å).

In TMS-F-DTPhz that crystallizes in the orthorhombic Pnma space group (Table 2), molecules occupy special positions on the mirror plane. The molecules form stacks along the [0 1 0] direction. The distance between planes of molecules in stacks is 3.48 Å. The crystal structure of TMS-Cl-DTPhz also consists of stacked molecules. The distances between planes of molecules in the stacks are 3.44 and 3.46 Å. In both structures, molecules pack in an antiparallel mode (Fig. 10), most favorable in the presence of bulky TMS substituents.

In the reported compounds, the interplanar distances in the stacking dimers range from 3.25 to 3.53 Å, which is consistent with values for analogous compounds, where such distances range from 3.25 to 3.61 Å. 69,70

The size and shape of Hirshfeld surfaces (HS) help identify intermolecular interactions and classify molecular crystals in terms of packing similarities. The CrystalExplorer program⁵⁵ was used to generate Hirshfeld surfaces and fingerprint plots in eight R-DTPhz (R = H, F, Cl, Br) compounds, taking into consideration in all cases the contents of the asymmetric units. The main contributions to

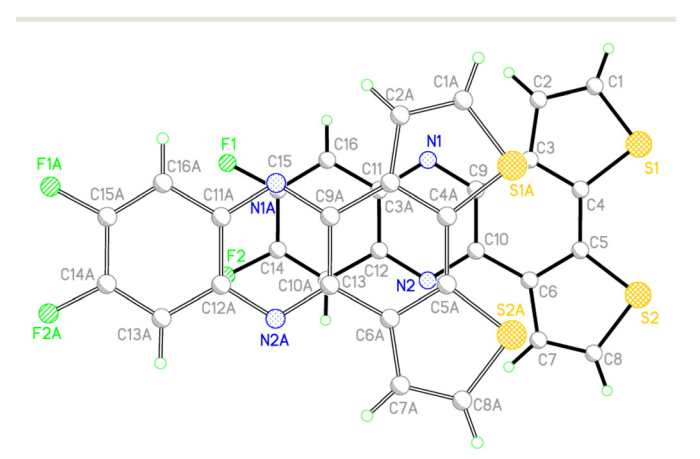


Fig. 7 An overlay scheme of the molecules in stacks in γ F-DTPhz. Symmetrically equivalent atoms are denoted with the suffix A.

the total HS areas are depicted by the d_{norm} surfaces (Fig. S1, S3, S5, S7, S9, S11, S13, and S15†) and by the full and decomposed fingerprint plots (Fig. S2, S4, S6, S8, S10, S12, S14, and S16 in the ESI†), and numerical values are summarized in Table S2.† It was evident that in the lack of strong donor centers in the molecules all the registered interactions were concentrated in the area of weak interactions with the predominant impact of those with H participation, like $H \cdots H$ and $H \cdots X$ (X = N, C, S, F, Cl, Br). In particular, H···H interactions comprised 35.7% and 34.6% in H-DTPhz polymorphs, with this value decreasing up to 18.8-23.0% in the halogen-substituted compounds (Table S2†) in favor of the impact of H···Hal interactions that varied in the range 10.8% (α Cl-DTPhz) to 19.3% (Br-DTPhz). The C···C contacts associated with π - π stacking interactions were registered with meaningful contributions, 7.5% (Br-DTPhz) to 15.0% (α F-DTPhz) in all compounds.

Computational analysis

Quantum chemical calculations showed that substituents at positions 9 and 10 in a series of H-DTPhz, F-DTPhz, and Cl-DTPhz do not have a significant effect on HOMO and LUMO wave functions, and both frontier orbitals are delocalized over whole π -systems (Fig. 11). The electron density on halogen atoms of F-DTPhz, Cl-DTPhz and Br-DTPhz is present in both HOMO and LUMO with stabilization of both frontier orbitals by approximately 0.2 eV in comparison with unsubstituted H-DTPhz, resulting in similar HOMO-LUMO gaps (Table 3). In addition, the first excitation energies for all molecules were calculated with the TD-DFT method (Table 3).

The calculated TD-DFT energy for H-DTPhz is almost the same as the electrochemical bandgap, 2.87 eV.⁴⁰ It should be mentioned that cyclic voltammetry analysis presented therein demonstrated that TMS groups have only a marginal impact on both half-wave reduction potentials of H-TMS-DTPhz (-1.80 V and -1.79 V for H-TMS-DTPhz and H-DTPhz respectively) and oxidation potentials (+1.06 and +1.08 V, respectively) with their difference for H-DTPhz equal to 2.87

Paper

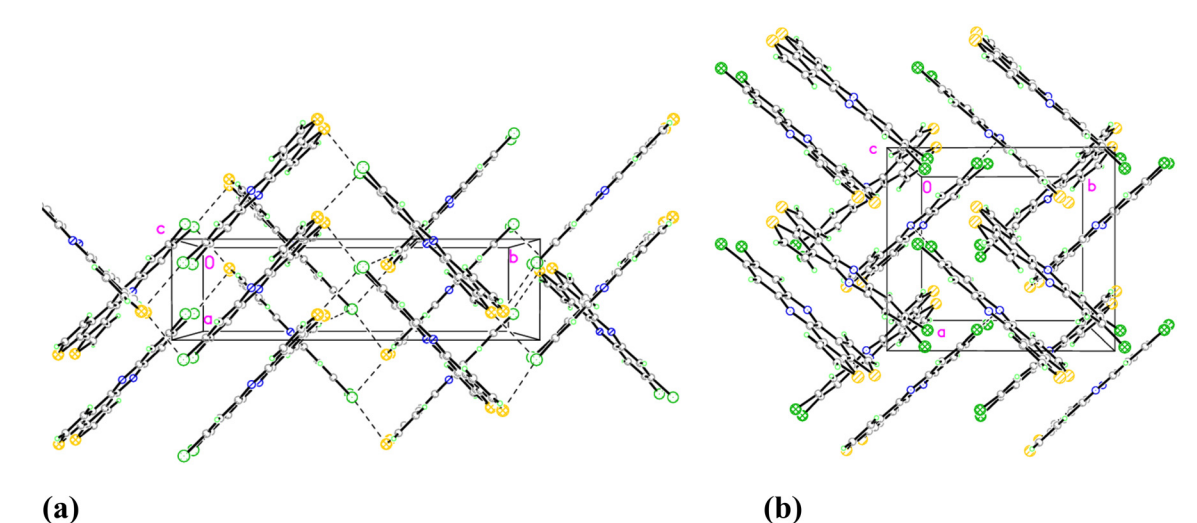


Fig. 8 The crystal structures of α Cl-DTPhz (a) and β Cl-DTPhz (b).

V and for **H-TMS-DTPhz** equal to 2.86 V. These results also agree with computational data presented in Table 3.

Crystal energy calculations of polymorphs

Results of X-ray studies demonstrated that **DTPhz** derivatives crystallize in seven different crystal packing types, I–VII, which correspond to experimental crystal structures of α H-DTPhz, β H-DTPhz, α F-DTPhz, β F-DTPhz, γ F-DTPhz, α Cl-DTPhz, and β Cl-DTPhz (which is also isomorphous to Br-DTPhz). To evaluate if all these packing types have some probability of realization for all four DTPhz derivatives (R = H, F, Cl, Br), lattice energy computations of these seven types for each R substituent were carried out using quantum-chemistry periodic plane-wave DFT and empirical force field methods (Table 4). In the case of experimental polymorphs, the X-ray crystal structures were used as initial models with

C–H bonds normalized to a standard distance of 1.09 Å. For the hypothetical structures, the halogen or hydrogen atoms of the experimental polymorph were substituted with R atoms of the corresponding R-DTPhz derivative. For example, for energy calculation of the polymorph of F-DTPhz with the crystal structure VI (α Cl-DTPhz), Cl atoms in α Cl-DTPhz were substituted with F atoms. For all calculated structures, the optimization of atomic coordinates and unit cell parameters was carried out.

The results of quantum chemical (PBE-D method) and force field (COMAPSS force field) calculations of relative energies for experimentally observed and hypothetical polymorphs are presented in Table 4; the energies that correspond to the experimentally found structures are presented in bold font. For both methods, the low-lying polymorphs correspond to experimentally observed structures. The quantum chemical calculations demonstrated

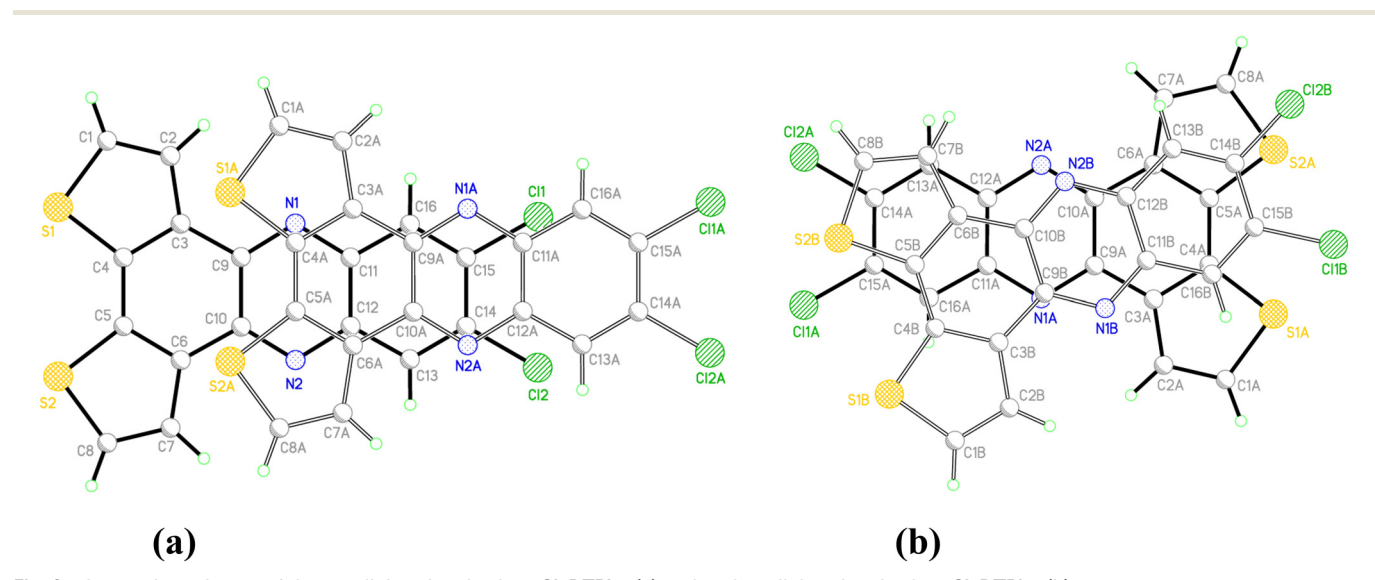


Fig. 9 An overlay scheme of the parallel molecules in α Cl-DTPhz (a) and antiparallel molecules in β Cl-DTPhz (b).

CrystEngComm **Paper**

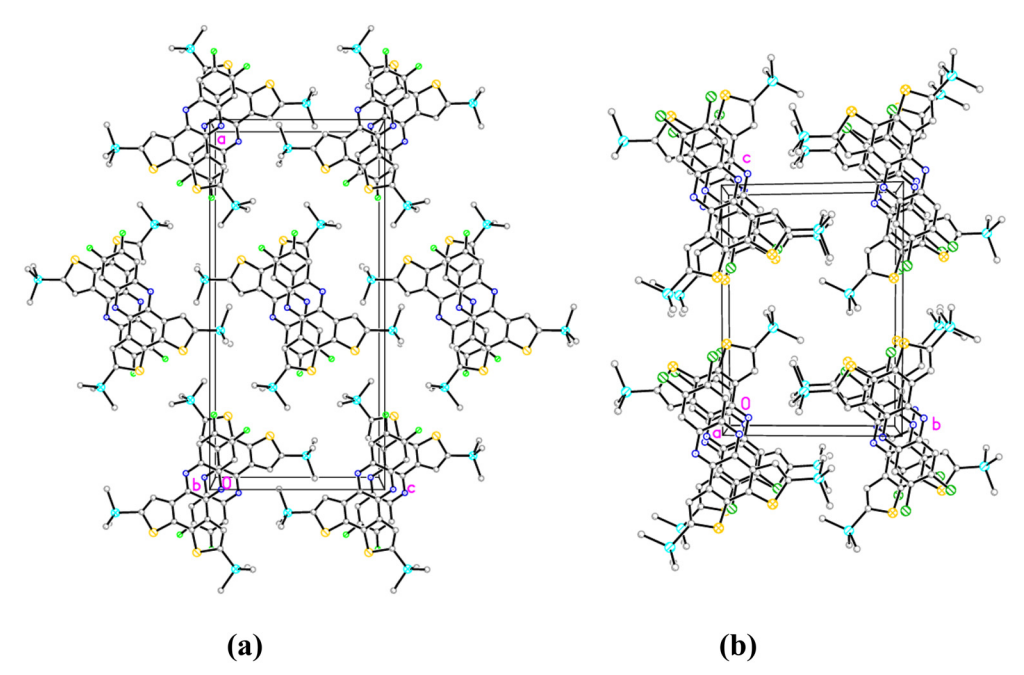


Fig. 10 Packing in the crystal structures of TMS-F-DTPhz (a) and TMS-Cl-DTPhz (b) demonstrating molecular stacks with antiparallel arrangement of molecules in both crystals.

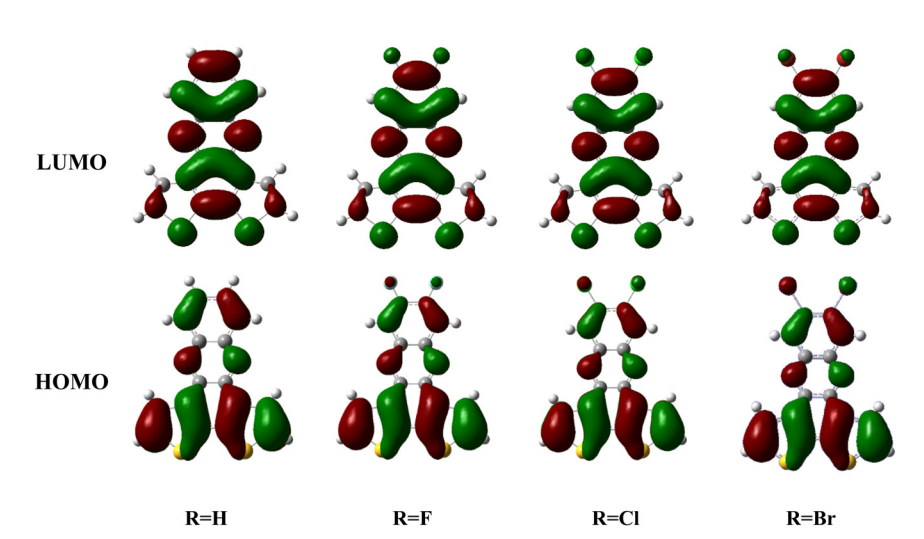


Fig. 11 Pictorial representations of the HOMO and LUMO wave functions of R-DTPhz (R = H, F, Cl, Br) as determined at the B3LYP/6-311G(d) level of theory.

Table 3	Theoretical	calculations	of orbital	energies i	n DTPhz	derivatives (eV)
---------	-------------	--------------	------------	------------	---------	------------------

	H-DTPhz	F-DTPhz	Cl-DTPhz	Br-DTPhz	F-TMS-DTPhz	Cl-TMS-DTPhz
B3LYP/6-311G((d)					
E_{HOMO}	-5.93	-6.10	-6.16	-6.14	-5.96	-6.01
E_{LUMO}	-2.56	-2.78	-2.92	-2.91	-2.70	-2.84
$E_{\rm gap}$	3.37	3.32	3.34	3.23	3.26	3.17
TD-DFT	2.85	2.79	2.71	2.70	2.73	2.64
M06/6-311G(d)						
E_{HOMO}	-6.20	-6.37	-6.41	-6.39	-6.23	-6.28
E_{LUMO}	-2.40	-2.62	-2.75	-2.73	-2.55	-2.68
$E_{ m gap}$	3.79	3.75	3.66	3.66	3.68	3.60
TD-DFT	2.95	2.90	2.82	2.82	2.84	2.76

0.0

4.7

4.3

1.3

0.7

Br

F

Cl

COMPASS force field

2.2

3.0

3.4

Polymorph VI VII Structure type β H-DTPhz α F-DTPhz β F-DTPhz γ F-DTPhz α Cl-DTPhz β Cl-DTPhz α H-DTPhz PBE-D Η 0.0 0.9 4.9 1.7 1.7 1.4 5.3 0.3 0.3 F 0.1 2..7 0.0 0.0 0.1 Cl 3.6 8.1 3.8 2.4 2.8 0.1 0.0

3.4

3.3

2.9

3.0

Table 4 The relative energies (kcal mol⁻¹) for seven types of polymorphs of R-DTPhz derivatives

0.6

4.4

4.8

a polymorphic diversity of the F-DTPhz compound, which is in agreement with experimental data. The calculated relative energies in the PBE-D method show that F-DTPhz has a high probability to crystallize in six of seven crystalline forms. Such behavior can be explained by the geometrical and electronic properties of the F-DTPhz molecule. Geometrically, it is similar to the H-DTPhz molecule, since the C-F bond distances (1.35 Å) are not much longer than C-H bond distances (1.09 Å), and at the same time its dipole moment (2.65 D) is close to the dipole moments of Cl-DTPhz (3.12 D) and Br-DTPhz (2.71 D). The relative energies for H-DTPhz show that in addition to experimentally observed polymorphs α and β (I and II polymorph type), it can also form three polymorphs with crystal packing of types IV-VI (structures of β F-DTPhz, γ F-DTPhz, and α Cl-DTPhz). The experimentally observed Cl-DTPhz polymorphs (structures VI and VII) are more than 2.0 kcal mol⁻¹ lower in energy than the hypothetical polymorphs. This can be explained by the geometric factor because the C-Cl distance, 1.72 Å, is much longer than the C-H and C-F distances. For Br-DTPhz, for which only one experimentally observed, PBE-D polymorph VII was calculations suggest a second possible polymorph corresponding to the structure of α Cl-DTPhz; both modeled structures VI and VII for Br-DTPhz have the same energies. This can be explained by the geometric (C-Br distance is 1.89 Å) and electronic similarities of both molecules.

COMPASS force field calculations show similar energy ranges for the polymorphs of H-DTPhz, Cl-DTPhz, and Br-DTPhz. For the H-DTPhz compound, the calculations also predict the possibility of polymorphs IV-VI. For the molecules of Cl-DTPhz and Br-DTPhz, only structures VI and VII correspond to low-lying polymorphs. For the F-DTPhz compound, COMPASS force field also predicts additional polymorphs; however, the calculated lattice energy for a F-**DTPhz** is 3.3 kcal mol⁻¹ higher than that for γ **F-DTPhz**, and thus α F-DTPhz should be unstable. Such a deficiency of calculations can be caused by the presence of six symmetrically independent molecules that significantly increases the number of variable parameters and complicates optimization.

4. Conclusions

0.0

0.0

2.6

3.6

0.5

1.2

2.3

2.7

Several new materials including dithieno[3,2-a:2',3'-c] phenazine and its 9,10-dihalogen derivatives (Hal = F, Cl, Br) with the general formula R-DTPhz have been characterized using experimental and computational methods. Crystals for X-ray diffraction analysis were prepared using solution and gas phase crystal growth methods, with and without the TCNQ coformer, which led to formation of seven packing polymorphs for three compounds with R = H, F and Cl. In spite of their similar molecular structure, all seven packing patterns are rather different, including two very uncommon crystal structures with 6 and 4 symmetrically independent molecules per asymmetric part of the unit cell (R = F). Results of quantum chemical calculations of lattice energy for H-, Fand Cl-substituted R-DTPhz polymorphs demonstrate that the low-lying polymorphs correspond to the experimentally observed structures. In all the studied compounds, π -stacked associates (dimers or stacks) with molecular interplanar distances below 3.5 Å were found that indicates, along with the voltammetric and computational data on HOMO-LUMO bandgaps, that they might be useful for formation of twocomponent co-crystals with stacked structure for potential applications in organic electronics. The most probable candidate to be employed in organic electronics seems to be γ F-DTPhz, whose structure and crystal shape are similar to characteristics found for a F-DTPhz, which is described in the literature as a crystalline elastic waveguide. 41

0.0

0.2

1.4

0.0

0.0

It should be mentioned that for compounds Br-DTPhz, TMS-F-DTPhz and TMS-Cl-DTPhz, only one polymorph was found experimentally; however, energy calculations of a series of crystal structures of these materials demonstrated a high probability of finding several more polymorphs for these compounds.

Author contributions

Conceptualization, B. B. A., T. V. T.; methodology, B. B. A.; investigation, B. B. A., R. C., E. V. J.; writing-original draft preparation, B. B. A., M. S. F., T. V. T.; writing-review and editing, all authors; visualization, all authors; funding

acquisition, T. V. T. All authors have read and agreed to the published version of the manuscript.

Conflicts of interest

The authors declare no conflict of interest.

Acknowledgements

We thank Y. Getmanenko for supplying us with materials which she synthesized during her employment as a postdoc at NMHU. We are grateful to Hui Jiang and Christian Kloc for assistance with crystal growth by the PVT method. The authors also gratefully acknowledge the Ohio Supercomputer Center for providing computational resources. This work was supported by the NSF via DMR-1523611 and DMR-2122108 (PREM). M. S. F. thanks the project ANCD 20.80009.5007.15 for support.

References

- 1 W. C. McCrone, in Physics and Chemistry of the Organic Solid State, ed. D. Fox, M. Labes and A. Weissenberg, Interscience Publishers, New York, 1965, vol. 2, p. 725.
- 2 J. Bernstein, Polymorphism in Molecular Crystals, Oxford University Press, Oxford, 2002.
- 3 in Crystal Engineering: The Design and Application of Functional Solids, ed. K. R. Seddon and M. Zaworotko, Kluwer Academic, 1999, vol. 539.
- 4 G. M. Day, A. V. Trask, W. D. S. Motherwell and W. Jones, Chem. Commun., 2006, 54-56.
- 5 F. J. J. Leusen and J. Kendrick, Polymorph Prediction of Small Organic Molecules, Co-crystals and Salts, Pharmaceutical Salts and Co-crystals, ed. J. Wouters, Royal Soc. of Chemistry, 2011, ch. 4, pp. 44-88.
- 6 C. Bodewig, Z. Kristallogr. Cryst. Mater., 1881, 5, 554-576.
- 7 P. K. Thallapally, R. K. R. Jetti, A. K. Katz, H. L. Carrell, K. Singh, K. Lahiri, S. Kotha, R. Boese and G. R. Desiraju, Angew. Chem., Int. Ed., 2004, 43, 1149-1155.
- 8 T. V. Timofeeva, G. H. Kuhn, V. V. Nesterov, V. N. Nesterov, D. O. Frazier, B. G. Penn and M. Y. Antipin, Cryst. Growth Des., 2003, 3, 383-391.
- 9 R. Castañeda, S. A. Antal, S. Draguta, T. V. Timofeeva and V. N. Khrustalev, Acta Crystallogr., Sect. E: Struct. Rep. Online, 2014, 70, 0924-0925.
- 10 E. H. Lee, Asian J. Pharm. Sci., 2014, 9, 163-175.
- 11 R.-Q. Song and H. Colfen, CrystEngComm, 2011, 13, 1249-1276.
- 12 G. Mehta, S. Sen and K. Venkatesan, CrystEngComm, 2007, 9,
- 13 G. Cavallo, P. Metrangolo, R. Milani, T. Pilati, A. Priimagi, G. Resnati and G. Terraneo, Chem. Rev., 2016, 116,
- 14 S. K. Seth, P. Manna, N. J. Singh, M. Mitra, A. D. Jana, A. Das, S. R. Choudhury, T. Kar, S. Mukhopadhyay and K. S. Kim, CrystEngComm, 2013, 15, 1285-1288.

- 15 K. Bechgaard, T. J. Kistenmacher, A. N. Bloch and D. O. Cowan, Acta Crystallogr., Sect. B: Struct. Crystallogr. Cryst. Chem., 1977, 33, 417-422.
- 16 T. J. Kistenmacher, T. J. Emge, A. N. Bloch and D. O. Cowan, Acta Crystallogr., Sect. B: Struct. Crystallogr. Cryst. Chem., 1982, 38, 1193-1199.
- 17 M. Courté, J. Ye, H. Jiang, R. Ganguly, S. Tang, C. Kloc and D. Fichou, Phys. Chem. Chem. Phys., 2020, 22, 19855-19863.
- 18 D. Gentili, M. Gazzano, M. Melucci, D. Jones and M. Cavallini, Chem. Soc. Rev., 2019, 48, 2502-2517.
- 19 S. Yan, A. Cazorla, A. Babuji, E. Solano, C. Ruzié, Y. H. Geerts, C. Ocal and E. Barrena, Phys. Chem. Chem. Phys., 2022, 24, 24562.
- 20 R. Bhowal and D. Chopra, Cryst. Growth Des., 2021, 21, 4162-4177.
- 21 M. L. Tang and Z. A. Bao, Chem. Mater., 2011, 23, 446-455.
- 22 H. Chung and Y. Diao, J. Mater. Chem. C, 2016, 4, 3915-3933.
- 23 Y.-G. Zhen, H.-L. Dong, L. Jiang and W.-P. Hu, Chin. Chem. Lett., 2016, 27, 1330-1338.
- 24 O. D. Jurchescu, D. A. Mourey, S. Subramanian, S. R. Parkin, B. M. Vogel, J. E. Anthony, T. N. Jackson and D. J. Gundlach, Phys. Rev. B: Condens. Matter Mater. Phys., 2009, 80, 085201.
- 25 L. A. Stevens, K. P. Goetz, A. Fonari, Y. Shu, R. M. Williamson, J.-L. Brédas, V. Coropceanu, O. D. Jurchescu and G. E. Collis, Chem. Mater., 2015, 27, 112-118.
- 26 J. A. Schneider, H. Black, H.-P. Lin and D. F. Perepichka, ChemPhysChem, 2015, 16, 1173-1178.
- 27 Q. Guo, L. Wang, F. Bai, Y. Jiang, J. Guo, B. Xu and W. Tian, RSC Adv., 2015, 5, 18875-18880.
- 28 G. Wesela-Bauman, S. Lulinski, J. Serwatowski and K. Wozniak, Phys. Chem. Chem. Phys., 2014, 16, 22762-22774.
- 29 H.-Z. Gao, Int. J. Quantum Chem., 2012, 112, 740-746.
- 30 F. Yu, G. Yang and Z. Su, Synth. Met., 2011, 161, 1073-1078.
- 31 W. Ratzke, L. Schmitt, H. Matsuoka, C. Bannwarth, M. Retegan, S. Bange, P. Klemm, F. Neese, S. Grimme, O. Schiemann, J. M. Lupton and S. Hoeger, J. Phys. Chem. Lett., 2016, 7, 4802-4808.
- 32 J. Z. Fan, Y. Zhang, C. L. Lang, M. Qiu, J. S. Song, R. Q. Yang, F. Y. Guo, Q. J. Yu, J. Z. Wang and L. C. Zhao, Polymer, 2016, 82, 228-237.
- 33 Y. Zhang, J. Y. Zou, H. L. Yip, K. S. Chen, J. A. Davies, Y. Sun and A. K. Y. Jen, Macromolecules, 2011, 44, 4752-4758.
- 34 M. L. Keshtov, S. A. Kuklin, N. A. Radychev, A. Y. Nikolaev, I. E. Ostapov, M. M. Krayushkin, I. O. Konstantinov, E. N. Koukaras, A. Sharmag and G. D. Sharma, Phys. Chem. Chem. Phys., 2016, 18, 8389-8400.
- 35 C. A. Richard, Z. X. Pan, H. Y. Hsu, S. Cekli, K. S. Schanze and J. R. Reynolds, ACS Appl. Mater. Interfaces, 2014, 6, 5221-5227.
- 36 C. A. Richard, Z. Pan, A. Parthasarathy, F. A. Arroyave, L. A. Estrada, K. S. Schanze and J. R. Reynolds, J. Mater. Chem. A, 2014, 2, 9866-9874.
- 37 X. Lu, T. Lan, Z. Qin, Z.-S. Wang and G. Zhou, ACS Appl. Mater. Interfaces, 2014, 6, 19308-19317.

- 38 T. H. El-Assaad, S. B. Shiring, Y. A. Getmanenko, K. M. Hallal, J. L. Bredas, S. R. Marder, M. H. Al-Sayah and B. R. Kaafarani, RSC Adv., 2015, 5, 43303-43311.
- 39 D. Yokoyama, H. Sasabe, Y. Furukawa, C. Adachi and J. Kido, Adv. Funct. Mater., 2011, 21, 1375-1382.
- 40 O. Ai, Y. A. Getmanenko, K. Jarolimek, R. Castañeda, T. V. Timofeeva and C. Risko, J. Phys. Chem. Lett., 2017, 8, 4510-4515.
- 41 M. Annadhasan, A. R. Agrawal, S. Bhunia, V. V. Pradeep, S. S. Zade, C. M. Reddy and R. Chandrasekar, Angew. Chem., Int. Ed., 2020, 59, 13852-13858.
- 42 X. Song, H. Yu, Y. Zhang, Y. Miao, K. Ye and Y. Wang, CrystEngComm, 2018, 20, 1669-1678.
- 43 X. Song, Z. Zhang, S. Zhang, J. Wei, K. Ye, Y. Liu, T. B. Marder and Y. Wang, J. Phys. Chem. Lett., 2017, 8, 3711-3717.
- 44 P. Brooks, D. Donati, A. Pelter and F. Poticelli, Synthesis, 1999, **1999**, 1303-1305.
- 45 Y. A. Getmanenko, C. Risko, P. Tongwa, E. G. Kim, H. Li, B. Sandhu, T. Timofeeva, J. L. Bredas and S. R. Marder, J. Org. Chem., 2011, 76, 2660-2671.
- 46 Y. A. Getmanenko, P. Tongwa, T. V. Timofeeva and S. R. Marder, Org. Lett., 2010, 12, 2136-2139.
- 47 Y. A. Getmanenko, M. Fonari, C. Risko, B. Sandhu, E. Galan, L. Y. Zhu, P. Tongwa, D. K. Hwang, S. Singh, H. Wang, S. P. Tiwari, Y. L. Loo, J. L. Bredas, B. Kippelen, T. Timofeeva and S. R. Marder, J. Mater. Chem. C, 2013, 1, 1467-1481.
- 48 R. A. Laudise, C. Kloc, P. G. Simpkins and T. Siegrist, J. Cryst. Growth, 1998, 187, 449-454.
- 49 Bruker-AXS; 2.2012.2 0 ed., Bruker AXS: Madison, Wisconsin, USA, 2009.
- 50 Bruker-AXS; 2014.11-0 ed., Bruker AXS: Madison, Wisconsin, USA, 2014.
- 51 G. M. Sheldrick, TWINABS Version 2012/1, An Empirical Correction for Absorption Anisotropy applied to Twinned crystals, Universität Göttingen, Göttingen, Germany.
- 52 G. M. Sheldrick, Acta Crystallogr., Sect. A: Found. Crystallogr., 2008, 64, 112-122.
- 53 G. M. Sheldrick, Acta Crystallogr., Sect. A: Found. Adv., 2015, 71, 3-8.
- 54 C. F. Macrae, I. J. Bruno, J. A. Chisholm, P. R. Edgington, P. McCabe, E. Pidcock, L. Rodriguez-Monge, R. Taylor, J. van de Streek and P. A. Wood, J. Appl. Crystallogr., 2008, 41, 466-470.
- 55 P. R. Spackman, M. J. Turner, J. J. McKinnon, S. K. Wolff, D. J. Grimwood, D. Jayatilaka and M. A. Spackman, CrystalExplorer: a program for Hirshfeld surface analysis, visualization and quantitative analysis of molecular crystals, J. Appl. Crystallogr., 2021, 54, 1006-1011.
- 56 M. J. Frisch, G. W. Trucks, H. B. Schlegel, G. E. Scuseria, M. A. Robb, J. R. Cheeseman, G. Scalmani, V. Barone, G. A. Petersson, H. Nakatsuji, X. Li, M. Caricato, A. Marenich, J. Bloino, B. G. Janesko, R. Gomperts, B. Mennucci, H. P.

- Hratchian, J. V. Ortiz, A. F. Izmaylov, J. L. Sonnenberg, D. Williams-Young, F. Ding, F. Lipparini, F. Egidi, J. Goings, B. Peng, A. Petrone, T. Henderson, D. Ranasinghe, V. G. Zakrzewski, J. Gao, N. Rega, G. Zheng, W. Liang, M. Hada, M. Ehara, K. Toyota, R. Fukuda, J. Hasegawa, M. Ishida, T. Nakajima, Y. Honda, O. Kitao, H. Nakai, T. Vreven, K. Throssell, J. A. Montgomery Jr., J. E. Peralta, F. Ogliaro, M. Bearpark, J. J. Heyd, E. Brothers, K. N. Kudin, V. N. Staroverov, T. Keith, R. Kobayashi, J. Normand, K. Raghavachari, A. Rendell, J. C. Burant, S. S. Iyengar, J. Tomasi, M. Cossi, J. M. Millam, M. Klene, C. Adamo, R. Cammi, J. W. Ochterski, R. L. Martin, K. Morokuma, O. Farkas, J. B. Foresman and D. J. Fox, Gaussian 09, Gaussian, Inc., Wallingford, CT, USA, 2009.
- 57 H. Sun, Compass, J. Phys. Chem. B, 1998, 102, 7338-7464.
- 58 P. Verwer and F. J. J. Leusen, Computer Simulation to Predict Possible Crystal Polymorphs, in Reviews in Computational Chemistry, John Wiley & Sons, Inc., 2007, p.
- 59 A. M. Rappe, K. M. Rabe, E. Kaxiras and J. D. Joannopoulos, Phys. Rev. B: Condens. Matter Mater. Phys., 1990, 41, 1227-1230.
- 60 S. Grimme, J. Comput. Chem., 2006, 27, 1787-1799.
- 61 V. Barone, M. Casarin, D. Forrer, M. Pavone, M. Sambi and A. Vittadini, J. Comput. Chem., 2009, 30, 934-939.
- 62 P. Giannozzi, S. Baroni, N. Bonini, M. Calandra, R. Car, C. Cavazzoni, D. Ceresoli, G. L. Chiarotti, M. Cococcioni, I. Dabo, A. Dal Corso, S. Fabris, G. Fratesi, S. de Gironcoli, R. Gebauer, U. Gerstmann, C. Gougoussis, A. Kokalj, M. Lazzeri, L. Martin-Samos, N. Marzari, F. Mauri, R. Mazzarello, S. Paolini, A. Pasquarello, L. Paulatto, C. Sbraccia, S. Scandolo, G. Sclauzero, A. P. Seitsonen, A. Smogunov, P. Umari and R. M. Wentzcovitch, Quantum Espresso: a modular and open-source software project for quantum simulations of materials, J. Phys.: Condens. Matter, 2009, 21, 395502.
- 63 C. R. Groom, I. J. Bruno, M. P. Lightfoot and S. C. Ward, Acta Crystallogr., Sect. B: Struct. Sci., Cryst. Eng. Mater., 2016, 72, 171-179.
- 64 C. F. Matta, J. Hernández-Trujillo, T.-H. Tang and R. F. W. Bader, Chem. - Eur. J., 2003, 9, 1940-1951.
- 65 V. R. Hathwar and T. N. Guru Row, Cryst. Growth Des., 2011, 11, 1338-1346.
- 66 V. R. Thalladi, H.-C. Weiss, D. Bläser, R. Boese, A. Nangia and G. R. Desiraju, J. Am. Chem. Soc., 1998, 120, 8702-8710.
- 67 K. Reichenbächer, H. I. Süss and J. Hulliger, Chem. Soc. Rev., 2005, 34, 22-30.
- 68 D. E. Arkhipov, A. V. Lyubeshkin, A. D. Volodin and A. A. Korlyukov, Crystals, 2019, 9, 242.
- 69 A. Putta, J. D. Mottishaw, Z. Wang and H. Sun, Cryst. Growth Des., 2014, 14, 350-356.
- 70 M. O. BaniKhaled, J. D. Mottishaw and H. Sun, Cryst. Growth Des., 2015, 15, 2235-2242.